Theor Chem Acc (2006) 116: 497–504
DOI 10.1007/s00214-006-0086-4

REGULAR ARTICLE

Tahra Ayed · Nathalie Guihéry
Bahoueddine Tangour · Jean-Claude Barthelat

Theoretical study of the metal–metal interaction in dipalladium(I) complexes

Received: 13 December 2004/Accepted: 14 May 2005 / Published online: 22 February 2006

Abstract Correlated ab initio calculations have been performed on three dipalladium(I) complexes. These compounds differ both by the metal–metal interaction and by the metal–ligand interaction. The $[Pd_2Cl_2(\mu-H_2PCH_2PH_2)_2]$ complex exhibits a σ overlap between the two binding metallic orbitals and has no bridging ligand. In $[Pd_2Cl_4(\mu-CO)_2]^{2-}$, the leading interaction between the two palladium involves a π overlap between the metallic orbitals and goes through the two bridging CO ligands. In $[Pd_2Cl_2(\mu-CO)(\mu-H_2PCH_2\ PH_2)_2]$, a single CO ligand bridges the two palladium atoms which interact through a hybrid σ–δ overlap. The three compounds also differ by the metal–metal distances. Surprisingly enough, while the palladium atoms are formally d^9 in all these complexes, none of them is paramagnetic. We propose here a detailed analysis of the electronic structures of these compounds and rationalize their chemical structures as well as the role of back-donation in the CO bridged compounds. Finally, since highly correlated treatments are used to describe these complexes, a detailed study of the role of both non-dynamical and dynamical correlations is performed. Concerning the $[Pd_2Cl_4(\mu-CO)_2]^{2-}$ complex, this analysis has revealed that the complex is not bound at the lowest correlated levels of calculation and therefore dynamical correlation is alone responsible for its binding energy.

Keywords Dipalladium(I) complexes · Metal–metal interaction · CASSCF method · DFT method

T. Ayed (✉) · N. Guihéry · J.-C. Barthelat
Laboratoire de Physique Quantique, IRSAMC/UMR5626, Université Paul Sabatier, 118 route de Narbonne, 31062 Toulouse Cedex 4, France
E-mail: ayed@irsamc.ups-tlse.fr

B. Tangour
Unité de Recherche de Chimie Théorique et Réactivité, Institut Préparatoire aux Etudes d'Ingénieur d'El Manar, Université de Tunis-El Manar, Tunis, Tunisia

1 Introduction

Dinuclear transition–metal complexes have attracted the interest of many organometallic and inorganic chemists. Their potential use for the conception of new magnetic materials or of compounds of biological interest justify this attention. Among them, compounds containing palladium(I) atoms have been extensively studied for their catalytic activity by experimentalists [1] On the other hand, only a few theoretical works [2,3] have been devoted to these compounds, even though their electronic structure is both interesting and quite difficult to determine from theoretical descriptions.

The *anti*-$[Pd_2Cl_2(\mu-dppmMe)_2]$ complex [4] (where dppmMe is 1,1-bis(diphenylphosphino)ethane) has no direct bridging ligand and the metal–metal distance has been measured from an X-ray diffraction study to be 2.664 Å. This complex will be modeled as $[Pd_2Cl_2(\mu-H_2PCH_2PH_2)_2]$ and will be referred to as complex **1**.

Concerning the $[Pd_2Cl_2(\mu-CO)(\mu-dppm)_2]$ complex (where dppm is bis(diphenylphosphino)methane), crystallographic data [5] show that the Pd atoms are bridged by a single CO group and that the Pd–Pd distance is 3.19 Å. On the basis of this Pd–Pd separation, a non-bonding metal–metal interaction has been suggested. Our study will deal with the model complex $[Pd_2Cl_2(\mu-CO)(\mu-H_2PCH_2PH_2)_2]$ which will be referred to as complex **2**.

Experimental studies [1] have shown that these dipalladium(I) complexes are diamagnetic, although the oxydation number of the palladium atoms is formally I, i.e., their electronic configuration is d^9. Another unusual feature is that, even though dinuclear metal carbonyl halides preferentially contain halogen rather than carbonyl bridges, the structures of CO bridged Pd(I) complexes are not consistent with this rule. From spectroscopic and crystallographical studies, Goggin et al. [6] found that the dianion $[Pd_2Cl_4(\mu-CO)_2]^{2-}$ (that will be referred to as complex **3**)is planar with the two CO groups bridging the Pd atoms. A theoretical study [7] of the electronic structure of this compound at the crystallographic geometry showed that a multicenter bond involving both the CO bridges and the Pd atoms is responsible for the

relatively short distance between the two metals. Calculations on several isomers involving bridging chlorides are also reported in ref. [7], but a strict comparison of their relative stability is inconclusive since the corresponding entities are not isoelectronic.

These questions are intrinsically interesting. From a theoretical point of view, the study of such compound is also challenging since

1. to address the question of the diradical versus the covalent character of such bonds, one should be able to treat non-dynamical correlation effects accurately;
2. a correct theoretical description of organometallic compounds also requires the treatment of dynamical correlation;
3. geometry optimizations using a high level of correlation are currently not possible.

Our interest was initially to investigate a series of dipalladium(I) complexes in order to determine the nature of the metal–metal interaction and the role of back-donation in the CO bridges. However, since the role of non-dynamical and dynamical correlation turned out to be crucial, a detailed study of the methods that are able to produce accurate results both on the geometrical structures and on the electronic properties of these complexes is presented.

Section 2 is devoted to a general presentation of the compounds studied. The different theoretical approaches that are used both for the determination of the electronic structures and their analysis are given in Sect. 3. Finally, a detailed discussion of the results is presented in Sect. 4. The specific effects of non-dynamical and dynamical correlation are also discussed in this section.

2 General presentation of the complexes studied

A schematical view of the complexes **1**, **2** and **3**, as well as the axes chosen, is given in Fig. 1a–1c, respectively.

Let us first concentrate on complex **1**. The ligand field removes the degeneracy of the d orbitals so that (according to the choice of the axes) the $d_{x^2-y^2}$ orbital of the Pd(I) atoms is the highest occupied metal-centered orbital. Since all the other Pd orbitals are filled, the leading metal–metal interaction goes through the σ overlap between the two $d_{x^2-y^2}$ orbitals of each Pd atom.

In complex **2**, the orbital of the Pd atoms which is destabilized by the ligand field is a hybrid orbital involving both the $d_{x^2-y^2}$ and the d_{z^2} atomic orbitals. The overlap between the two $d_{x^2-y^2}$ is of δ nature while there is a slight σ overlap between the two d_{z^2} contributions to these orbitals. The resulting overlap has a mixed δ–σ character. This complex contains a single CO bridge that is expected to participate in the metal–metal interaction. The highest occupied molecular orbital (HOMO) of free CO is a carbon lone pair designated as σ_{CO}, while the lowest unoccupied molecular orbital (LUMO) is an antibonding orbital of π character between the two atoms that will be designated as π^*_{CO}.

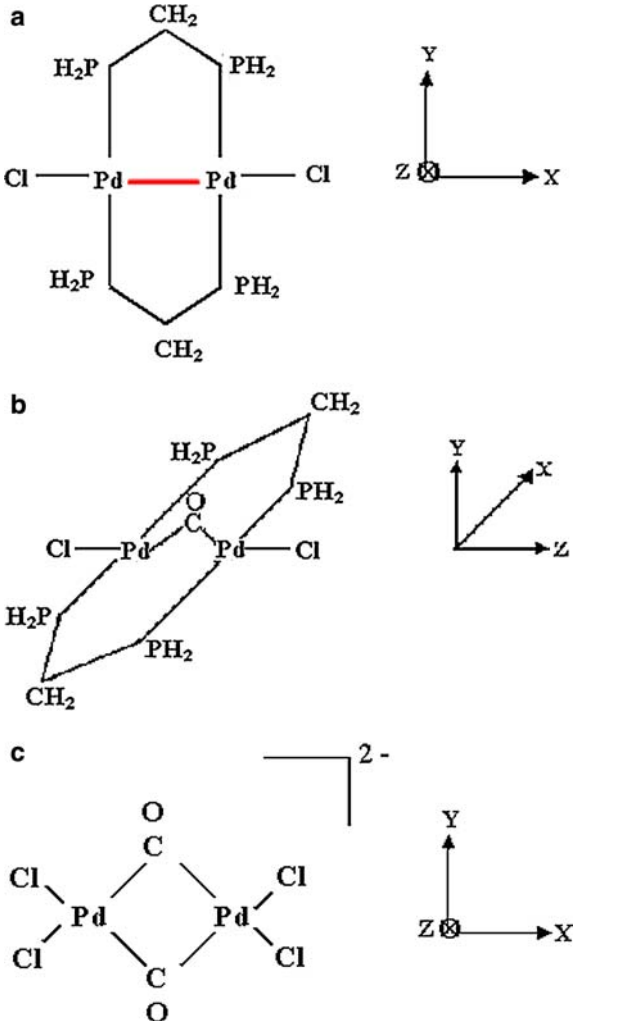

Fig. 1 **a** Schematic view of complex **1**. **b** Schematic view of complex **2**. **c** Schematic view of complex **3**

Concerning complex **3**, the highest occupied atom-centered orbital of the Pd atom is the d_{xy} orbital. The metal–metal interaction goes through the π overlap between these two orbitals. Of course, this interaction also involves the CO bridging ligands [7]. Since the distance between them is large enough, we can ignore the ligand–ligand interaction. Only compatible symmetry-adapted combinations of the σ_{CO} orbitals and of the π^*_{CO} orbitals can interact with the metal-centered orbitals. Let us call σ^-_{CO} the antibonding combination of the σ_{CO} orbitals and π^{*-}_{CO} the antibonding combination of the π^*_{CO}. These are the combinations which interact with the Pd orbitals.

3 Theoretical approaches and tools for the determination and analysis of the electronic and nuclear structures

As previously explained, the palladium atoms are formally Pd(I) and therefore exhibit a d^9 electronic configuration. The distance between the two metallic atoms seems to be large

enough to raise the question of the ability of a single-determinantal wave function to describe the Pd–Pd interaction. Although the three compounds studied have been found experimentally to be diamagnetic, a correlated description is necessary for a full understanding of their electronic structure, i.e., for a correct evaluation of the diradical–covalency ratio of the metal–metal interaction. In order to optimize the charge fluctuation in the two above-mentioned metal-centered orbitals, a complete active space (CAS) calculation restricted to two electrons in two orbitals was carried out. Larger active spaces have also been considered and calculations show that the minimal CAS, i.e., two electrons in two orbitals is sufficient for an adequate description of all the complexes studied. Dynamical correlation is then taken into account through difference dedicated configuration interaction (DDCI) [9] calculations as explained further.

While calculations are generally performed using delocalized symmetry-adapted (SA) orbitals, the interpretation of the electronic structure is much easier in localized (atom-centered) orbitals [8]. Let us call p and m the SA linear combinations of the atomic orbitals. The optimized bonding and antibonding p and m orbitals have tails on the surrounding ligands, but are essentially of metallic character. Starting from these orbitals one may define left and right orbitals a and b that are metal-centered and orthogonal by the following equations:

$$a = \frac{p+m}{\sqrt{2}}, \tag{1}$$

$$b = \frac{p-m}{\sqrt{2}}. \tag{2}$$

In a single-determinantal method, the determinant that should be the most appropriate for the desccription of the system is

$$\phi_0 = |\text{core} \cdot p\bar{p}|, \tag{3}$$

if p is lower in energy than m. Its physical content is given by its expression as a function of the atom-centered orbitals

$$\phi_0 = |\text{core} \cdot \frac{1}{2}(a\bar{a} + b\bar{b} + a\bar{b} + b\bar{a})|. \tag{4}$$

In this approach, it is thus clear that the weights of the neutral valence bond (NVB) forms $a\bar{b}$ and $b\bar{a}$ and ionic valence bond (IVB) forms $a\bar{a}$ and $b\bar{b}$ are equal. But for a system in which the two atoms are far enough from each other (as it is the case here), such a determinant is not adequate. An accurate description of the electronic structure must reproduce the prevalence of the NVB forms over the ionic ones. CAS calculations are required to relax the weight of these NVB forms. For a singlet state, the Ψ_{CAS} wave function involves also another reference which is:

$$\phi_0' = |\text{core} \cdot m\bar{m}| \tag{5}$$

The CASSCF procedure optimizes both the coefficients λ and μ of the references in the singlet $\psi^{\text{S}}_{\text{CAS}}$ wave function and the molecular orbitals (MO) in order to minimize the energy. $\Psi^{\text{S}}_{\text{CAS}}$ can be written as

$$\Psi^{\text{S}}_{\text{CAS}} = \lambda p\bar{p} - \mu m\bar{m}, \tag{6}$$

where λ and μ are positive. The weights of the neutral and ionic VB forms are now not constrained to be equal, as can be seen in the following expression:

$$\Psi^{\text{S}}_{\text{CAS}} = \frac{\lambda+\mu}{2}|\text{core} \cdot a\bar{b}+b\bar{a}| + \frac{\lambda-\mu}{2}|\text{core} \cdot a\bar{a}+b\bar{b}|. \tag{7}$$

The weights of the neutral and ionic VB forms can be used to measure the covalency of a bond. Let us define the covalency index C as the ratio of the IVB forms to the NVB:

$$C = \frac{(\lambda-\mu)^2}{(\lambda+\mu)^2}. \tag{8}$$

For a strictly covalent bond, the two weights are identical and the covalency will be equal to one while for a strongly correlated bond, i.e., exhibiting a strict diradicalar character ($\lambda = \mu$), this ratio will be equal to zero. The values of the covalent indices of the three compounds will be calculated and compared to the Wiberg indices that are evaluated from the density matrices calculated at the density functional theory (DFT) level.

One should note that another way of looking at the greater or smaller diradicalar character of a bond is to evaluate the excitation energy to the lowest triplet state. This state has only a neutral VB structure in the spin component $S_z = 1$ and is given by the following expression:

$$\Psi^{\text{T}} = |\text{core} \cdot pm| = |\text{core} \cdot ab|. \tag{9}$$

The CASSCF method that introduces the non-dynamical correlation furnishes only a zeroth order description and, as already observed in the study of many organometallic compounds, the evaluation of dynamical correlation is also necessary. We have therefore performed extensive CI calculations. The relative position of the singlet and triplet states has been studied using the DDCI method [9]. This CI is specially designed for the treatment of energy differences between states of the same CAS and has been successfully applied to a large number of magnetic compounds [10–12]. The excited determinants involved in the CI are all the single and all the double excitations that imply up to one hole and two particles or two holes and one particle. The analysis of the correlated wave function gives several types of information. The weight of the NVB and IVB forms as well as the occupation of the natural orbitals (O_{HOMO} and O_{LUMO} for the natural HOMO and LUMO orbitals, respectively) are of course modified by the effect of dynamical correlation.

The calculations reported here were performed using the MOLCAS package [13] for the CASSCF step and using the CASDI package [14] for the CI one.

In order to determine the geometrical structures of the compounds, a method that correctly describes their electronic structure, i.e., that includes both the non-dynamical and the dynamical correlation, is necessary. In practice, there is no single method available that has such a level of sophistication. We have, therefore, used both DFT and CASSCF optimization procedures. DFT calculations were performed with the Gaussian 98 series of programs [15] using the B3LYP hybrid functional [16, 17]. Quasi-relativistic energy-adjusted pseudopotentials determined by Dolg et al. [18] were used to represent the Pd-like core. The 18 electrons corresponding to the

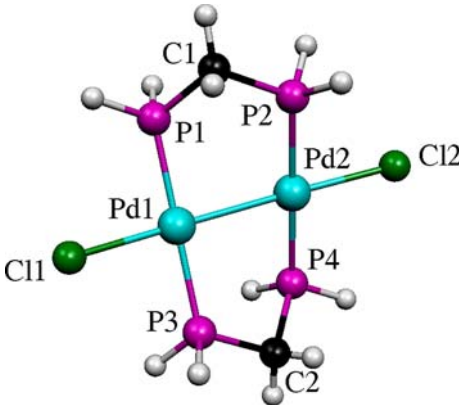

Fig. 2 Geometrical structure of complex **1** optimized at the DFT/B3LYP level

$4s, 4p, 4d$ and $5s$ Pd orbitals were described by a $(8s, 7p, 6d)$ primitive set of Gaussian functions contracted to $(6s, 5p, 3d)$.

While the CASSCF method does not produce reliable structures as shown in Sect. 4, the DFT optimized geometries compare quite well with experiment. In order to validate the use of the DFT method, the binding energy of the multicenter bond that appears in complex **3** has also been calculated using both DFT and DDCI methods (see Sect. 4.2).

4 Results and discussion

The main structural parameters of the optimized geometries are given in Tables 1, 2 and 3 and compared to X-ray data. The main results concerning the electronic structures are reported in Table 4 (for the Wiberg and covalency indices) and Table 5 (for the CASSCF and DDCI results). This section is organized as follows. The electronic structures are discussed in Sect. 4.1. All the geometry optimizations were performed at the DFT level. In order to check whether this method is relevant for the determination of the geometrical structures of the compounds studied, correlated calculations were performed on the complex **3**. The corresponding results are presented in Sect. 4.2.

4.1 Electronic structures

Let us first concentrate on complex **1**. The main geometrical parameters optimized at the DFT/B3LYP level are reported in Table 1 and the optimized structure is represented in Fig. 2. These parameters compare well with the X-ray data of the *anti*-$[Pd_2Cl_2(\mu-dppmMe)_2]$ complex. A slight overestimation of the optimized distances can be noted which is comparable to the usual overestimation observed for DFT/B3LYP geometry optimizations. The Pd–Pd distance is quite short, supporting the idea of a single σ bond between the two Pd atoms.

Concerning the electronic structure, the metal–metal interaction goes effectively through the σ overlap of the two $d_{x^2-y^2}$ orbitals, as can be seen in Fig. 3 where the HOMO and LUMO orbitals of the complex are represented. The weights of the two references at both CASSCF and DDCI levels of calculation are reported in Table 5. Even if the singlet wave function is dominated by a single determinant, the weight of the second reference is quite substantial, showing that this system is correlated. It should be noticed that this weight is lowered by the effect of dynamical correlation, as is usually observed in magnetic or correlated systems [19]. As a consequence, the weight of the ionic VB forms increases. The covalency index is 0.59 at the DDCI level, suggesting that a correlated σ bond exists between the two Pd atoms. This result is consistent with the non-negligible occupation of the LUMO natural orbital (0.12 electron). Concerning the Wiberg indices reported in Table 4, we can see that the Pd–Pd Wiberg bond index is the highest one (in comparison with those of the other complexes) but it is very low compared to the value obtained from the correlated ab initio study. Even if the role of non-dynamical correlation is not negligible, this system is only partially correlated and the covalency between the Pd atoms is quite important.

Concerning compound **2**, the main geometrical parameters are given in Table 2 and they compare well with the X-ray data of the $[Pd_2Cl_2(\mu-CO)(\mu-dppm)_2]$ complex. The optimized geometry is represented in Fig. 4. The distance beween the two Pd atoms is quite large (3.19 Å) and suggests that there is no bonding interaction between the two atoms.

The electronic structure obtained at both CASSCF and DDCI levels of calculation is dominated by a single reference. It is interesting to note that here again the weight of the second reference is not negligible suggesting a correlated bond. In contrast to what is expected from the Pd–Pd distance, there is a multicenter bond involving both the Pd atoms and the bridging CO ligand. The HOMO and LUMO orbitals are represented in Fig. 5. Surprisingly enough, the HOMO results from an antibonding interaction between the Pd atoms. The bonding interaction with the π^*_{CO} is responsible for the stabilization of the symmetry-adapted antibonding combination. In contrast, the LUMO orbital results from the bonding interaction between the two Pd atoms and is destabilized by an antibonding interaction with the σ_{CO}. The σ donation and π back-donation of the CO bridge explain this quite unusual energetic ordering of the orbitals. The weights of the neutral and ionic VB forms are given in Table 5 and can be compared to those of the other complexes. It can be noted that this system is the least correlated one, in contrast to what is expected. This bond happens to be the most covalent one ($C = 0.67$) and the occupation of the natural LUMO orbital is the lowest, although it is non-negliglible. Concerning the Wiberg index, the corresponding value is the lowest (in comparison with the other complexes). This result is in complete contradiction with the analysis of the correlated wave function. The incoherence of this value in this case is attributable to the definition of the Wiberg index itself. Indeed, the Wiberg index is an overlap population and is therefore proportional to the overlap between the orbitals of the concerned atoms. In the case considered, the two atoms are spatially far apart

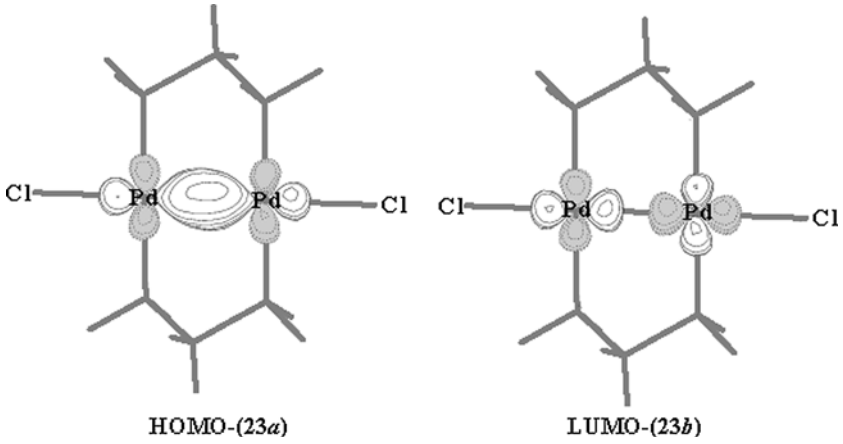

Fig. 3 HOMO and LUMO CASSCF orbitals of complex **1**

and their interacting orbitals produce a hybrid δ–σ overlap which is probably very small.

The fairly long Pd–Pd distance deserves some discussion. The bonding interaction between the orbitals of the Pd atoms and the π^*_{CO} is favored when the angle Pd–C–Pd is larger, since the σ overlap between the orbitals involved on the Pd atoms and those of the bridging CO increases. This interaction therefore increases as the separation between them increases. However, the dppm bridges constrain the two Pd atoms to stay quite close. The resulting geometrical conformation is a compromise between a linear situation in which the σ overlap between the Pd orbitals and the π^*_{CO} would be maximal and a minimal steric hindrance with the external dppm bridges. The strong participation of the CO group in the correlated wave function is in agreement with the quite long CO bond distance, reflecting the importance of the back-donation.

The optimized geometrical parameters of compound **3** are given in Table 3 and it is represented in Fig. 6. One should note that the DFT optimized geometry is puckered while the crystallographic one is planar. The geometry of this complex in solution is known to be puckered as well [6], and we can reasonably think that the planarity of the crystal is due to packing effects and to the Madelung field. The Pd–Pd distance is a little longer than the crystallographic one and is comparable to the value in compound **1**. For this specific compound, we performed correlated calculations in order to better understand the electronic structure and to validate the use of the DFT method for geometry optimization (this will be discussed in Sect. 4.2).

Concerning the electronic structure, both CASSCF and DDCI calculations reveal here again the prevalence of a single reference in the singlet wave function. The weight of the second reference is however large enough to consider that the system is correlated. This result is also corroborated by the substantial occupation of the natural LUMO orbital. The HOMO and LUMO orbitals are represented in Fig. 7. The HOMO confirms the multicenter bond already observed by Kostic and Fenske [7] and constituted of an antibonding interaction between the two Pd atoms and a bonding interaction with the π^{*-}_{CO}. The LUMO results from a bonding interaction between the Pd atoms and an antibonding interaction between the metal-centered orbitals and the σ^{-}_{CO} orbitals. The σ donation and π back-donation are responsible for thisunusual electronic structure. The covalence (0.61) of the Pd–Pd bond is intermediate between those of the two other complexes. It is interesting to note that the presence of two bridging CO does not increase the strength of the interaction between the two Pd atoms, despite what is expected. The overlap between the π^{*-}_{CO} and the metal-centered orbitals is probably less important here than in the previous complex, due to the smaller value of the Pd–C–Pd angle. The Pd–Pd Wiberg index is here also too small to account for the binding character of the interaction showing that this index is not appropriate for the description of multicenter bonds. Finally when looking at the weight C_{CAS} of the references in the correlated wave function, we see that this weight is the lowest one compared to the two other complexes, thereby highlighting the very important role of dynamical correlation in this complex, as discussed in Sect. 4.2 devoted to the geometrical structures.

4.2 Geometrical structures

This subsection is exclusively devoted to the complex **3** and deals with the level of correlation required for an adequate

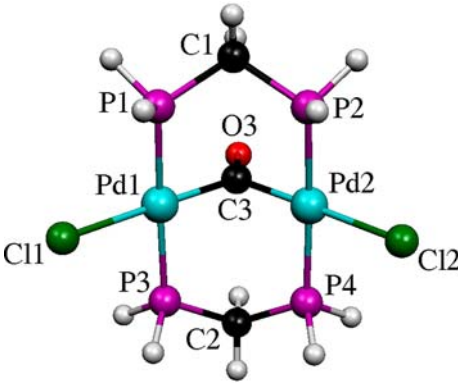

Fig. 4 Geometrical structure of complex **2** optimized at the DFT/B3LYP level

Table 1 Structural parameters[a] of the model complex $[Pd_2Cl_2(H_2PCH_2PH_2)_2]$ **1** optimized at the DFT/B3LYP level of calculation and X-ray data for *anti*-$[Pd_2Cl_2(dppmMe)_2]$

	DFT/B3LYP	X–ray[b]
Pd_1–Pd_2	2.696	2.664(1)
Pd_1–Cl_1	2.436	2.401
Pd_2–Cl_2	2.436	2.420
Pd_1–P_1	2.307	2.297
Pd_2–P_4	2.307	2.294
Pd_1–P_3	2.301	2.297
Pd_2–P_2	2.301	2.294
P_1–C_1	1.873	1.839
P_4–C_2	1.873	1.862
P_2–C_1	1.866	1.849
P_3–C_2	1.866	1.861
$P_{1(3)}$–$C_{1(2)}$–$P_{2(4)}$	103.6	106.5–105.9
$Cl_{1(2)}$–$Pd_{1(2)}$–$Pd_{2(1)}$	177.1	177.5–177.0
P_1–Pd_1–P_3	180.0	175.5
P_2–Pd_2–P_4	180.0	173.4
Cl_1–Pd_1–Pd_2–Cl_2	15.4	–
P_1–Pd_1–Pd_2–P_2	29.4	–
P_1–P_2–P_3–P_4	−45.5	–

[a]Distances are in Å and angles in degrees
[b]Ref. [4] (Standard deviations are available only for Pd_1–Pd_2)

Table 2 Structural parameters[a] of the model complex $[Pd_2Cl_2(\mu\text{-}CO)(H_2PCH_2PH_2)_2]$ **2** optimized at the DFT/B3LYP level of calculation and X-ray data for $[Pd_2Cl_2(\mu{-}CO)(\mu{-}dppm)_2]$

	DFT/B3LYP	X-ray[b]
Pd_1–Pd_2	3.193	3.190(4)
$Pd_{1(2)}$–$Cl_{1(2)}$	2.447	2.427(1)–2.445(1)
$Pd_{1(2)}$–C_3	2.020	1.971(4)–1.974(4)
$Pd_{1(2)}$–$P_{1(2)}$	2.355	2.340(1)–2.335(1)
$Pd_{1(2)}$–$P_{3(4)}$	2.355	2.341(1)–2.336(1)
C_3–O_3	1.194	1.184(5)
$Cl_{1(2)}$–$Pd_{1(2)}$–C_3	178.6	174.8(1)–178.8(1)
$P_{1(2)}$–$Pd_{1(2)}$–$P_{3(4)}$	174.7	171.33(4)–171.48(4)
$Pd_{1(2)}$–C_3–O_3	127.8	125.27(5)–126.79(5)
$P_{1(2)}$–$Pd_{1(2)}$–C_3	90.7	86.5(1)–86.1(1)
$P_{3(4)}$–$Pd_{1(2)}$–C_3	90.7	85.8(1)–87.1(1)
Pd_1–C_3–Pd_2	104.4	107.93(5)
Cl_1–Pd_1–Pd_2–Cl_2	0.0	–
C_1–C_3–O_3–C_2	180.0	–

[a]Distances are in Å and angles in degrees
[b]Ref. [5]

description of geometrical structures of correlated compounds. Of course, one of its objects is to check the ability of the DFT method to describe correctly the electronic structure of correlated compounds and therefore to produce accurate geometrical structures. The very good agreement between the geometrical parameters optimized for the other complexes and the X-ray data comforted us in thinking that DFT geometry optimizations can reasonably be used for the description of the compound studied. Moreover, although the DFT does not take the effect of the non-dynamical correlation explicitly into account, the prevalence of a single determinant and the inclusion of correlation through an exchange-correlation functional lead to a correct description of such systems.

Table 3 Structural parameters[a] of the complex $[Pd_2Cl_4(\mu\text{-}CO)_2]^{2-}$ **3** optimized at the DFT/B3LYP level of calculation and determined by X-ray data

	DFT/B3LYP	X-ray[b]
Pd_1–Pd_2	2.750	2.697(3)
Pd_1–C_1	2.033	1.994(9)
Pd_1–Cl_1	2.445	2.372(4)
C_1–O_1	1.167	1.140(10)
Pd_1–C_1–Pd_2	85.1	85.2(3)
C_1–Pd_1–C_2	90.3	–
Cl_1–Pd_1–Cl_3	93.4	–
Cl_1–Pd_1–C_1	88.1	–
Pd_1–C_1–O_1	137.1	–
C_1–Pd_1–Pd_2–C_2	148.4	–

[a]Distances are in Å and angles in degrees
[b]Ref. [6]

Table 4 Covalency indices *C* calculated at the DDCI level for the Pd–Pd interaction and Wiberg bond indices *W* evaluated from NBO analysis on the three complexes studied

Complex	**1**	**2**	**3**
$C(Pd_1$–$Pd_2)$	0.59	0.67	0.61
$W(Pd_1$–$Pd_2)$	0.325	0.069	0.153
$W(Pd_{1(2)}$–$P_{1(4)})$	0.453	0.382	–
$W(Pd_{1(2)}$–$P_{3(2)})$	0.442	0.382	–
$W(Pd_{1(2)}$–$Cl_{1(2)})$	0.250	0.265	0.302
$W(Pd_{1(2)}$–$Cl_{3(4)})$	–	–	0.302
$W(Pd_{1(2)}$–$C_{1(2)})$	–	–	0.522
$W(Pd_{1(2)}$–$C_{2(1)})$	–	–	0.522
$W(Pd_{1(2)}$–$C_3)$	–	0.534	–
$W(P_{1(4)}$–$C_{1(2)})$	0.921	0.908	–
$W(P_{2(3)}$–$C_{1(2)})$	0.897	0.908	–
$W(C_{1(2)}$–$O_{1(2)})$	–	–	2.030
$W(C_3$–$O_3)$	–	1.861	–

It is interesting to note that a geometry optimization of this compound at the CASSCF level leads to four separated fragments, namely two CO molecules and two $PdCl_2^-$ anions. In order to see whether complex **3** is bound and at what level of calculation it should be described, we have performed non-correlated and correlated calculations. Unexpectedly, this complex can be optimized at the RHF level of calculation. The corresponding geometry is relatively close to the DFT one. However, when calculating the energies of the separated fragments (at the ROHF level for the $PdCl_2^-$ fragments and at the RHF level for CO), it turns out that the molecule is not bound, i.e. the sum of the energies of the fragments is lower than the energy of the optimized geometry of the complex. The separated fragments are bound only by the multicenter bond that goes through the bridging CO. The appearance of a well in the potential energy surface at the RHF level is a pure artefact that is due to the incorrect dissociation of the single-determinantal wave function which constrains the weights of the NVB and IVB forms to be equal. Even if the dissociation energy is lower than the artefactual energy well, the optimization procedure that maintains this wave function along the dissociation parameter cannot dissociate properly. When using the CASSCF procedure, the weight of the NVB forms is increased and the system can dissociate properly.

Table 5 Main results obtained at the CASSCF and DDCI levels of correlation for the three model complexes

	Complex **1** CASSCF	DDCI	Complex **2** CASSCF	DDCI	Complex **3** CASSCF	DDCI
ΔE^{a}	38.0	52.0	43.0	50.0	50.0	77.0
λ^{b}	0.947	0.9913	0.971	0.9953	0.957	0.9924
μ^{b}	0.321	0.1293	0.238	0.0972	0.290	0.1239
C^{c}_{CAS}	1.00	0.89	1.00	0.89	1.00	0.86
NVB[d]	0.804	0.630	0.731	0.597	0.777	0.629
IVB[d]	0.196	0.370	0.269	0.403	0.222	0.377
O^{e}_{HOMO}	1.794	1.896	1.887	1.900	1.832	1.893
O^{e}_{LUMO}	0.206	0.116	0.113	0.099	0.168	0.105

[a]Energy difference (kcal mol^{-1}) between the singlet ground state and the first triplet excited state
[b]Values of the coefficients of the main determinants in the ground state wave function
[c]Weight of the renormalized references of the CASSCF in the ground state wave function
[d]Weights of the neutral (NVB) and ionic (IVB) forms in the ground state wave function
[e]Occupations of the HOMO and LUMO natural orbitals

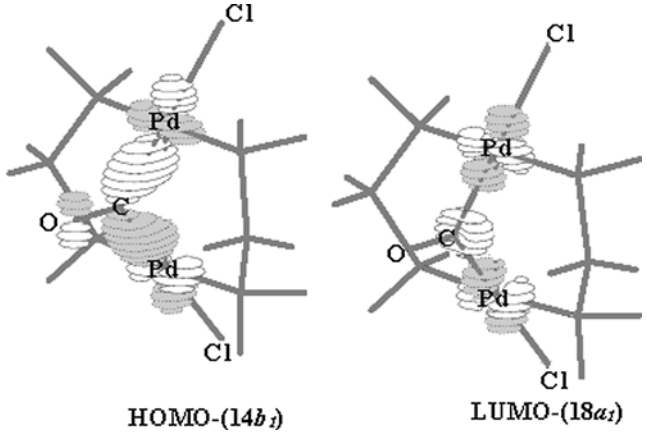

Fig. 5 HOMO and LUMO CASSCF orbitals of complex **2**

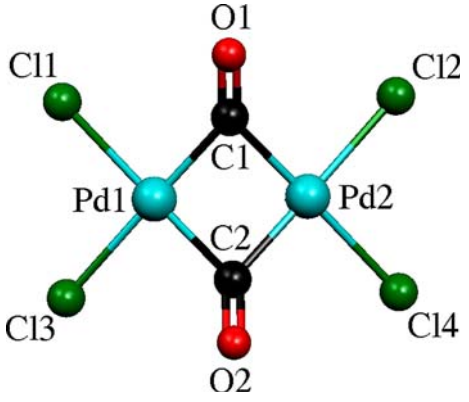

Fig. 6 Geometrical structure of complex **3** optimized at the DFT/B3LYP level

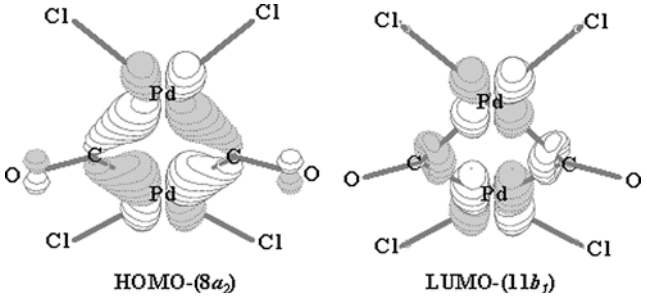

Fig. 7 HOMO and LUMO CASSCF orbitals of complex **3**

However, as already noticed for the two other complexes, the weight of the NVB forms, compared to the IVB ones is exagerated by the CASSCF wave function which represents only a zeroth-order description of such systems. The inclusion of dynamical correlation through the DDCI algorithm restores a correct ratio of the IVB versus NVB forms. The increase of the IVB forms is due to the inclusion of dynamical polarization effects [8]; these favor the occurrence of double occupancies of the metal-centered orbitals and therefore lead to a more covalent bond. Such a qualitative change of the geometrical structures observed at the CASSCF versus dynamically correlated methods has already been observed. For instance, the potential energy well in the F_2 molecule is increased by almost 1 eV when adding to the CAS, the singly excited determinants on all the references [20,21]. The most famous case concerns the Cr_2 molecule which is bounded by 1.47 eV experimentally [22] and 1.49 eV at the CAS + second-order perturbation theory level [23] while the potential energy curve is repulsive at the CAS(12,12) SCF level.

The fragmentation energy (energy difference between the molecule at its equilibrium geometry and two CO groups and two $PdCl_2^-$ anions in their frozen geometry) has been calculated at the DFT and DDCI levels. The potential well is estimated to be 50 kcal mol^{-1} at the DDCI level of correlation and 53 kcal mol^{-1} at the DFT level. It is interesting to note that the two values compare very well, demonstrating the relevance of the DFT method for the geometry optimization of such complexes.

5 Conclusion

Three different complexes of dipalladium atoms have been studied. One of the ambiguities of these complexes is due to the apparent contradiction between the electronic configuration of the Pd atoms that are formally d^9 and their

diamagnetic character. The Wiberg bond index and the covalency index of the Pd–Pd bond have been evaluated in order to discuss this specific point. Their geometrical and electronic structures have been determined using both DFT and highly correlated ab initio calculations. While DFT calculations furnish reliable geometrical structures and energies, they do not provide any indication concerning the magnitude of the diradicalar character of the bonds involved. A full understanding of the electronic structures of these complexes requires the use of correlated methods. For this purpose, DDCI calculations that are generally used for the description of magnetic compounds have been carried out. This study has shown that

1. all complexes are dominated by a single reference determinant which, since the total number of electron is even, results in the pairing of all electrons. However, the wave function is partially correlated in all cases and the role of non-dynamical correlation is crucial to obtain a suitable zeroth-order description. The role of dynamical correlation turns out also to be very important and a correct estimate of a covalency index requires extended CI calculations.
2. these complexes differ by the Pd–Pd distance, the Pd–Pd orbital overlap and the number of bridging ligands. While the Pd–Pd interaction in compound **1** results in a through-space σ bond, compounds **2** and **3** contain a multicenter bond that goes through the bridging CO groups. Unexpectedly, compound **2** for which the distance between the two Pd atoms is the largest appears to be the most covalent complex, while compound **1** which exhibits a direct σ bond is the most diradicalar.
3. Wiberg indices are too small and do not account for the binding character of the Pd–Pd interaction, whether it is through space or through bond. Moreover, the resulting bond order is in complete contradiction with the covalency indices determined at a more correlated level of treatment. This last index reproduces correctely the circulation of the electrons between the atoms involved in the bond and their binding interaction.
4. in the complexes studied, the geometrical structures are such that a strong bonding interaction between the Pd atoms prevents them from being paramagnetic. The bridging CO are responsible for a through-bond interaction that would not take place in Cl-bridged compound for a hypothetical isoelectronic complex. In compound **2**, this interaction is favored by the opening of the Pd–C–Pd angle which results in a larger distance between the Pd atoms.
5. the determination of the geometrical structure of compound **3** is quite difficult. The DFT method furnishes both a reliable geometry and a correct estimate of the binding energy. While the HF method converges on a spurious suspended well (although qualitatively in agreement with experimental data) , the CASSCF method dissociates the complex into four separated fragments. Finally, it has been found that dynamical correlation only is responsible for its binding character.

Acknowledgements We deeply thank Professor Colin Marsden for helpful discussions.

References

1. Murahashi T, Kurosawa H (2002) Coord Chem Rev 231:207 and references therein
2. Dedieu A (2000) Chem Rev 100:543
3. Mealli C, Ienco A, Galindo A, Carreno EP (1999) Inorg Chem 38:4620
4. Besenyei G, Párkányi L, Gács-Baitz E, James BR (2002) Inorg Chim Acta 327:179
5. Blin J, Braunstein P, Fischer J, Kickelbick G, Knorr M, Morise X, Wirth T (1999) J Chem Soc, Dalton Trans 2159
6. Goggin PL, Goodfellow RJ, Herbert IR, Orpen AG (1981) J Chem Soc Chem Commun 1077
7. Kostic NM, Fenske RF (1983) Inorg Chem 22:666
8. Guihéry N, Malrieu JP, Evangelisti S, Maynau D (2001) Chem Phys Lett 349:555
9. Miralles J, Castell O, Caballol R, Malrieu JP (1993) Chem Phys 172:33
10. Moreira I de PR, Illas F, Calzado CJ, Sanz JF, Malrieu JP, Ben Amor N, Maynau D (1999) Phys Rev B59:R6593
11. Castell O, Caballol R (1999) Inorg Chem 38:668
12. Calzado CJ, Cabrero J, Malrieu JP, Caballol R (2002) J Chem Phys 116:2728
13. Roos BO, Taylor PR, Siegbahn PEM (1980) Chem Phys 48:157
14. Ben Amor N, Maynau D (1998) Chem Phys Lett 286:211
15. Frisch MJ, Trucks GW, Schlegel HB, Scuseria GE, Robb MA, Cheeseman JR, Zakrzewski VG, Montgomery JA Jr, Stratmann RE, Burant JC, Dapprich S, Millam JM, Daniels AD, Kudin KN, Strain MC, Farkas O, Tomasi J, Barone V, Cossi M, Cammi R, Mennucci B, Pomelli C, Adamo C, Clifford S, Ochterski J, Petersson GA, Ayala PY, Cui Q, Morokuma K, Salvador P, Dannenberg JJ, Malick DK, Rabuck AD, Raghavachari K, Foresman JB, Ciolowski J, Ortiz JV, Baboul AG, Stefanov BB, Liu G, Liashenko A, Piskorz P, Komaroni I, Gomperts R, Martin RL, Fox DJ, Keith T, Al-Laham MA, Peng CY, Nanayakkara A, Challacombe M, Gill PMW, Johnson B, Chen W, Wong MW, Andres JL, Gonzalez C, Head-Gordon M, Replogle ES, Pople JA (2001) GAUSSIAN98 Revision A.11, Gaussian Inc., Pittsburgh, PA
16. Becke AD (1993) J Chem Phys 98:5648
17. Lee C, Yang W, Parr RG (1988) Phys Rev B 37:785
18. Andrea D, Haeussermann U, Dolg M, Stoll H, Preuss H (1990) Theor Chim Acta 77:123
19. Guihéry N, Malrieu JP (2003) J Chem Phys 119:8956
20. Hiberty PC (1992) Chem Phys Lett 189:259
21. Ghailane R, Lepetit MB, Malrieu JP (1993) J Phys Chem 97:94
22. Casey SM, Leopold DG (1993) J Phys Chem 97:816
23. Angeli C, Cimiraglia R, Malrieu JP (2002) J Chem Phys 117:9138